Comparison of atmospheric correction algorithms for deriving sea surface temperature from AVHRR

M. L. STEYN-ROSS*, D. A. STEYN-ROSS and A. JELENAK

Department of Physics and Electronic Engineering, Room E3-20,
The University of Waikato, Gate 8, Hillcrest Road, Private Bag 3105,
Hamilton, New Zealand

Abstract. Methods used to infer sea surface temperatures (SSTs) from satellite have traditionally been based on regression-tuned split-window fixed-coefficient algorithms. These can give inaccurate SST results when local atmospheric conditions are significantly different from those encapsulated by the regression averaging. The new generation of SST algorithms attempts to correct for atmospheric variability. These approaches include the R_{54} transmittance-ratio methods of other workers, and the dynamic water vapour (DWV) correction method of the authors. The relative performances of the various methods are compared by applying each to an ocean and satellite dataset obtained off the west coast of Tasmania, Australia in 1987. We also investigate the performance of the NESDIS operational multi-channel, cross-product, and nonlinear formulas for NOAA-9, -11, -12, and -14 when applied to the same dataset. We find the DWV method gives SST retrievals which have significantly smaller bias errors than those returned by the three transmittance-ratio methods. The best overall performance was returned by the NESDIS multichannel (MCSST) formula for NOAA-9, indicating that in low water vapour loading situations, the standard regression-based algorithms work well.

1. Introduction

The infrared channels of the AVHRR (advanced very high resolution radiometer) carried by the NOAA (National Oceanic and Atmospheric Administration) series of satellites have been used to infer sea surface temperatures (SSTs) on a global basis for well over two decades. More recently, the same technology has been utilized in the acquisition of land surface temperatures (LSTs).

In general, algorithms involve linear combinations of satellite brightness temperatures observed in channels 4 and 5 (centred near 11 and $12\,\mu$m respectively), and follow the so-called split-window (McMillin 1975) form:

$$T_s = T_4 + A(T_4 - T_5) + B \qquad (1)$$

where T_4 and T_5 are the satellite brightness temperatures of channels 4 and 5. The constants A and B are most commonly found by regressing in-situ surface data with

---

*e-mail: msr@waikato.ac.nz

coincident satellite data; or by using synthetic data for surface temperature and AVHRR signal, manufactured by ingesting atmospheric profiles into a radiative transfer model. We use the phrase 'fixed-coefficient split-window' to classify this type of algorithm which implicitly assumes that it is possible to use the same regression constants over a wide temporal and spatial extent.

Many different variations of the split-window form have been applied to the retrieval of land and sea surface temperatures (LSTs and SSTs) from satellites. For reviews of current LST methods see Prata (1993), and for SST methods see Barton (1995). For SST retrievals, the assumption of fixed-coefficients (and constant atmosphere) in the split-window formalism is the main source of error because of local atmospheric fluctuations. To overcome this, it is standard practice to periodically update the coefficients using ocean buoys to provide surface truth. As an alternative to this *in situ* tuning approach, a new generation of atmospherically correcting algorithms has been developed: the transmission ratio methods of Harris and Mason (1992) and Sobrino *et al.* (1993, 1994); and the dynamic water vapour (DWV) correction method of Steyn-Ross *et al.* (1993, 1997). The transmission ratio methods are all based on the notion that the atmospheric profile is constant over an area where the surface temperature may change. These methods implement a split-window algorithm in which A is modified by the inclusion of a transmittance ratio,

$$R_{54} = \frac{\tau_5}{\tau_4} \tag{2}$$

where 4 and 5 refer to the corresponding AVHRR infrared channels; τ is the atmospheric transmittance for a given channel. The effect of including R_{54} in the A-coefficient of (1) is to increase the magnitude of the atmospheric correction as the atmosphere becomes optically thicker. (Details of these methods and their rationale are given in §2.)

In contrast, the DWV method does not assume the atmosphere is constant over a given spatial extent. Rather, it allows for local atmospheric fluctuations (notably in the water content) and corrects for these by dynamically tuning the atmospheric profile. The method employs a full radiative transfer approach. A local radiosonde is required to provide a first-guess atmospheric profile. The water vapour content is then tuned until the pair of SST estimates retrieved from channels 4 and 5 are equal.

The DWV approach to the problem of SST determination from satellite radiance is conceptually equivalent to that used to retrieve atmospheric profiles of temperature and molecular composition: given a set of observed satellite radiances, what is the optimal atmospheric profile which minimizes the differences between the predicted radiances (as found by ingesting the profile into a suitable atmospheric model) and the actual radiances?

This problem has been tackled by many workers. The physical methods of Chahine (1970) and Smith (1970) apply the equation of radiative transfer to retrieve atmospheric temperatures located at the peaks of weighting functions, iterating from a first-guess profile until convergence is detected.

The inverse-matrix methods (Rodgers 1976; Eyre 1987, 1989) linearize the equations of transfer about a first-guess atmospheric profile and cast them into matrix form. If the transmission is assumed to be independent of temperature, then the matrix equation is linear in temperature deviation about the first-guess values. The temperature profile can then be retrieved by inverting the matrix equation using a

minimum variance technique. However, when the interaction and inter-dependence of atmospheric components need to be considered, the inverse problem becomes nonlinear, and, as described by Rodgers (1976), becomes one of estimation: what are the appropriate criteria which determine the optimum solution for a given set of observations?

The DWV approach attempts to solve the nonlinear estimation problem using a physical approach similar to that of Chahine (1970) and Smith (1970). At each iteration, DWV adjusts the atmospheric profiles by a set amount, then recalculates the transmissivities for each channel. The algorithm is presented in detail in §3, with the relevant equations given in the appendix.

Central to the estimation problem is the choice of 'forward' model: given the atmospheric profiles, how does one compute the at-satellite radiances? For our work, we ran the LOWTRAN-7 (Kneizys *et al.* 1988) atmospheric model. A referee has reminded us of the shortcomings in the LOWTRAN-7 treatment of the water vapour continuum; however, because we used LOWTRAN-7 in our original DWV investigations (Steyn-Ross *et al.* 1993), as did Sobrino *et al.* (1993, 1994) in theirs, we chose to retain LOWTRAN-7 for the present study, thus ensuring consistency in the comparisons. For future studies we intend running more up-to-date models which include a more accurate treatment of molecular absorption (e.g. CKD 2.2, Han *et al.* 1997).

The authors applied the DWV method over sea (Steyn-Ross *et al.* 1993) using data obtained off the west coast of Tasmania; and over land (Steyn-Ross *et al.* 1997) utilizing FIFE-89 data from an intensive Kansas grasslands field experiment (Strebel *et al.* 1992, 1994). When compared with a standard fixed coefficient split-window algorithm, the method was found to give a significant improvement in retrieval accuracy.

In the present paper we compare the relative performance of the DWV method with that of the transmission ratio algorithms due to Harris and Mason (1992) and Sobrino *et al.* (1993, 1994). Also compared are a selection of eight NESDIS operational SST algorithms. We use the same Tasmanian data set as used in our 1993 study. In our earlier work, we found that DWV sometimes failed to produce a reasonable surface temperature. Subsequent sensitivity studies showed that the method was prone to error if the first-guess atmospheric temperature profile was significantly higher than the actual temperature profile. To overcome this limitation, we have revised the DWV algorithm to tune the atmospheric temperature profile in those cases for which water vapour tuning does not produce convergence. We refer to the tuning of atmospheric temperature as DAT (dynamic atmospheric temperature); the umbrella term DWVT (dynamic water vapour and atmospheric temperature) is used to indicate that either the water vapour or the temperature profile may be tuned.

2. Variable-coefficient split-window algorithms

The three methods described below attempt to compensate for atmospheric variability by replacing the fixed A-coefficient of the traditional split-window form (1) with a variable coefficient which incorporates the R_{54} transmittance ratio (2).

2.1. *H&M: Harris and Mason (1992)*

Harris and Mason applied the Zavody (Rutherford Appleton Laboratory, UK) radiative transfer model to a suite of 56 ocean radiosonde profiles to compute the

at-satellite AVHRR brightness temperatures in channels 4 and 5 for nadir viewing. (Harris and Mason did not identify which AVHRR filter functions were used; from the date of their work it seems likely they used NOAA-11.) By regressing $(T_s - T_4)$ against $(T_4 - T_5)$, Harris and Mason derived a conventional SST algorithm of the form given in (1) with coefficients $A = 2.681$, $B = -0.15$. They then observed that the rms residual error could be significantly improved by arranging that the A-coefficient, which scales the $(T_4 - T_5)$ correction, be increased as the atmosphere becomes optically thicker. They found that the ratio of transmittances in channels 5 and 4, $R_{54} = \tau_5 / \tau_4$, provided a suitable weighting factor, resulting in a new transmittance-ratio split-window algorithm

$$T_s = T_4 + \frac{1.755}{R_{54}}(T_4 - T_5) + 0.38 \tag{3}$$

whose rms residual for the simulation set was 0.12 K. (Harris and Mason also developed a 4-coefficient regression fit, but we judged the 0.01 K improvement in rms residual not to be significant, so chose not to implement it for these tests.)

2.2. *Sob93: Sobrino* et al. *(1993)*

Sobrino *et al.* (1993) continued the Harris and Mason philosophy of including explicitly, via the R_{54} transmittance ratio, the effect of variable optical depth on the split-window coefficients. Using a set of 60 radiosoundings which cover the worldwide variability of SST (250–315 K) and atmospheric moisture (0.2–6.7 g cm^{-2}), they considered three observation angles (0°, 23°, 46°) and three surface temperatures for a total of 540 simulated geophysical situations. The resulting (T_4, T_5) NOAA-11 AVHRR brightness temperature pairs were computed with LOWTRAN-7 (Kneizys *et al.* 1988). Their simulation study produced the following 4-coefficient split-window SST algorithm:

$$T_s = T_4 + (2.301/R_{54} - 0.16)(T_4 - T_5) - 4.20/R_{54} + 4.61 \tag{4}$$

giving a standard error of 0.27 K for the 540 simulation points.

2.3. *Sob94: Sobrino* et al. *(1994)*

Sobrino *et al.* (1994) investigated the generalization of the transmittance-ratio split-window technique to the more difficult problem of LST determination. Using NOAA-11 filter functions, the same representative set of 60 radiosondes (described above for Sob93), three observation angles, 49 surface emissivity combinations $(\varepsilon_4, \varepsilon_5$ ranging from 0.9 to 1.0, with $\Delta\varepsilon$ ranging from -0.02 to 0.02), and five surface temperatures, a total of 44 100 (T_4, T_5) situations were simulated. Their resulting LST algorithm was presented as a radiance formulation:

$$B_4(T_s) = \left(\alpha_1 + \frac{\alpha_2}{R_{54}}\right)B_4(T_4) + \left(\alpha_3 + \frac{\alpha_4}{R_{54}}\right)B_4(T_5) + \left(\alpha_5 + \frac{\alpha_6}{R_{54}}\right) \tag{5}$$

where $B_4(T)$ is the channel-4 blackbody radiance at temperature T, and the α_i $(i = 1 \ldots 6)$ are functions of surface emissivities ε_4 and ε_5. Since for the present SST tests we can set $\varepsilon_4 = \varepsilon_5 = 1$, the emissivity dependence inherent in the α_i coefficients of (9) disappears, so that (9) becomes equivalent to an SST algorithm stated in radiance space. For this idealized case, the α coefficients simplify to the emissivity-independent constants listed in column 1 of their Table V: $\alpha_1 = -0.4048$, $\alpha_2 = 3.3074$, $\alpha_3 = 1.4928$, $\alpha_4 = -3.3771$, $\alpha_5 = 0.1416 \times 10^{-6}$, $\alpha_6 = -0.2264 \times 10^{-6}$.

Although not stated in their paper, it is clear that while α_1 through α_4 are dimensionless, coefficients α_5 and α_6 must carry units of radiance. Sobrino *et al.* used LOWTRAN-7 for their radiative transfer calculations, so we presume that (5) is written for the default LOWTRAN blackbody radiance unit of $W/(cm^2\,sr\,cm^{-1})$. Since we choose to work in the standard NOAA/NESDIS radiance units of $mW/(m^2\,sr\,cm^{-1})$, we scaled the listed values for α_5 and α_6 by a multiplicative factor of 10^7.

3. DWVT: Dynamic Water Vapour and Temperature algorithm

The original DWV method (Steyn-Ross *et al.*, 1993) was found to have shortcomings and has now been superseded by DWVT. In this section we briefly describe DWV, then give details of the new DWVT algorithm. The equations and rationale for dynamic tuning of the atmospheric temperature and water vapour profiles are presented in the appendix.

DWV uses the equation of radiative transfer for channels 4 and 5 of the AVHRR in the mean-value approximation (appendix equation A1). Given observed satellite radiances and an initial guess for the atmospheric profile, the relative humidity is shifted by a constant fraction at each level until the same SST is predicted by the equation of transfer for both channels. Central to the original DWV philososphy is the assumption that atmospheric uncertainties are due to water vapour fluctuations only; thus during the water vapour adjustment, the atmospheric temperature at each level is left unchanged from the first-guess values.

However, our 1993 analysis revealed that, for some of the satellite passes, DWV produced SST estimates which were much too low. From sensitivity tests, we deduced that these failures could be attributed to the first-guess temperature profile (from non-local radiosonde) being too warm. The at-satellite signal is the sum of the surface radiance (attenuated by the intervening atmosphere) plus that arising from the atmosphere itself. If the assumed atmosphere is warmer than actual, the at-satellite contribution from the atmosphere will be artificially raised, so that the surface contribution must be reduced. DWV responds by increasing the water vapour amount (to reduce the transmission of the surface signal) thereby depressing the apparent surface temperature.

It was to handle this too-warm atmosphere case that DWVT was developed. DWVT allows tuning either of the water vapour profile or of the atmospheric temperature profile. DWVT proceeds as follows:

1. Establish atmospheric profile. If this is the first iteration, take the profile obtained from a nearby radiosonde as the first-guess atmosphere. Otherwise use the adjusted atmosphere produced by the tuning in step 5 (or 6) below.
2. Compute atmospheric variables. Initialize the LOWTRAN-7 transmittance code with this atmosphere, and hence compute τ_4, τ_5, and $\bar{T}_a$.
3. Solve for SST_4, SST_5. Using the known at-satellite radiances I_4 and I_5, and the computed atmospheric variables, apply equation (A3) (in appendix) to calculate two independent estimates for the surface temperature, SST_4 and SST_5.
4. Test for convergence. If $SST_4 = SST_5$, we have retrieved the surface temperature $T_s = SST_4 = SST_5$. If $SST_4 \neq SST_5$, then the assumed atmospheric state is in error, and should be tuned, either in water vapour (step 5), or, if necessary, in temperature profile (step 6).

5. DWV: Tune RH profile

5a. Adjust RH$_i$. Adjust (increase or decrease) the relative humidity at each level i by a fractional amount Δ_{RH}:

$$RH'_i = (1 + \Delta_{RH}) \cdot RH_i \qquad (6)$$

(Adjusted relative humidity is never allowed to exceed the saturation figure of 100%.)

5b. Iterate DWV. Repeat steps 1 to 5a, ensuring that the $(SST_4 - SST_5)$ difference steadily diminishes with each iteration.

5c. Test for DWV failure. If the sequence of differences stops converging (i.e. starts to increase, or shows a constant difference), then DWV is about to fail, so halt water vapour adjustment, and switch to atmospheric temperature adjustment (step 6).

6. DAT: Tune T_{atm} profile

6a. Adjust $T_{a,i}$. Restore the water vapour profile to its first-guess values. Replace step 5a with the corresponding temperature profile shift for each level i:

$$T'_{a,i} = (1 + \Delta_T) \cdot T_{a,i} \qquad (7)$$

where Δ_T is a constant fraction (of the absolute temperature).

6b. Iterate $T_{a,i}$ adjustments. Repeat steps 1–4, 6a until $SST_4 = SST_5$.

6c. Test for convergence failure. If no convergence is detected, settle on that profile adjustment which minimizes the $(SST_4 - SST_5)$ difference, taking the average as the retrieved surface temperature, $T_s = (SST_4 + SST_5)/2$.

Figure 1 shows a sample DWV run for a particular AVHRR observation (30 July 1987) over the buoy pixel. The SST_4/SST_5 estimates converged after the atmospheric water vapour (relative humidity) at each sonde level had been increased by $\times 1.6$.

For the case illustrated in figure 2, DWV failed to converge, so DAT was invoked, producing convergence when the atmospheric temperature (in Kelvin) at each sonde level had been reduced by 3.5% from the first-guess sonde values.

4. Operational fixed-coefficient split-window algorithms

To round out the method comparisons, we used our NOAA-9 and buoy dataset to compare the relative performance of eight operational SST retrieval formulas which have been developed by NESDIS for NOAA-9, -11, -12, and -14. We ask the question: how large are the retrieval errors when NOAA-9 brightness temperatures from our 1987 Tasmanian dataset are applied to the various operational algorithms developed for the later NOAA satellites?

Ideally the AVHRR instruments carried on different NOAA satellites would be identical so that an SST algorithm developed for say, NOAA-9, might be expected to work equally well on a later satellite. However, there are subtle instrument-to-instrument differences in the channel-4 and -5 bandpass characteristics (and therefore in the published central wavenumber values). In addition, SST algorithm coefficients depend on the average atmospheric state which prevailed during the time of the buoy-vs-satellite temperature regressions. For these two reasons, the operational split-window algorithms vary both with satellite and with time. Nevertheless, it is of interest to know just how consistent the various operational algorithms are.

The methods we selected for testing are drawn from Appendix E of the NOAA Polar Orbiter Data User's Guide, published on the World Wide Web at:
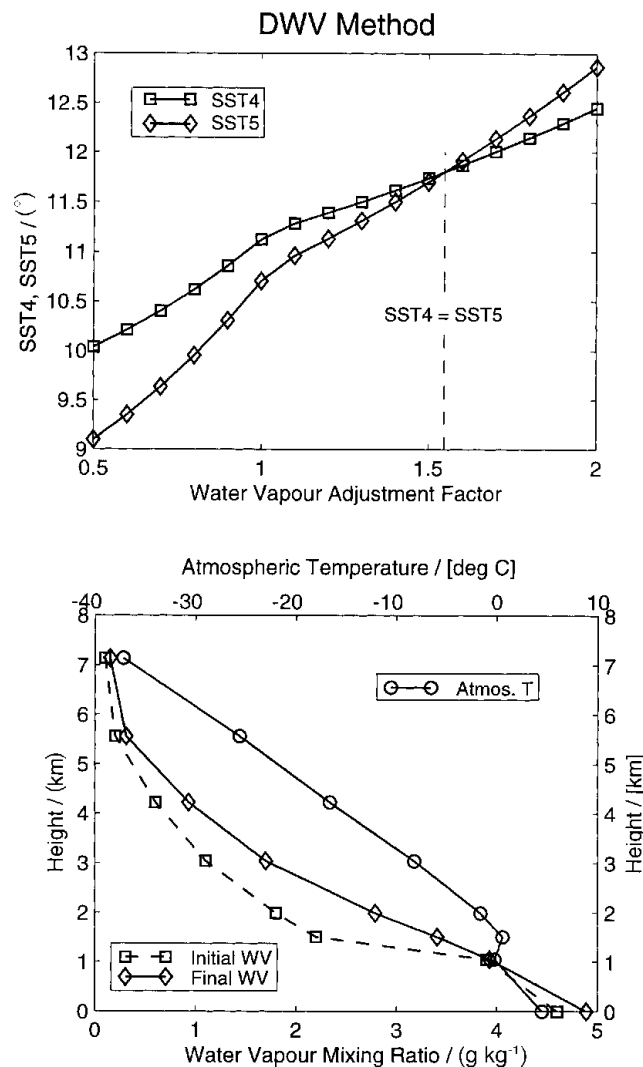
Figure 1. DWV method: SST retrieval via water vapour tuning. (*a*) The pair of SST predictions from AVHRR channels 4 and 5 match when the radiosonde-derived relative humidity at each level has been increased by a factor of 1.6, giving a DWV prediction of 11.9°C (the buoy reading was 11.8°C). (*b*) First-guess and tuned atmospheric profiles. The upper solid curve (circles) shows variation of atmospheric temperature (upper axis) with altitude. Dashed curve (squares) shows initial water vapour profile (lower axis), while middle solid curve (diamonds) shows final tuned water vapour profile obtained after relative humidity at each level has been increased by factor 1.6. These curves apply to satellite pass mafw (30 July 1987).

http://perigee.ncdc.noaa.gov/docs/podug/html/e/app-e.htm. For each satellite we selected representative algorithms (multichannel, cross-product, nonlinear) which were both operational and closest in time to our 1987 dataset. By 'operational', we mean that the equation was either used operationally by NESDIS to derive SST values, or was a close relative which formed part of the bundle of equations published by NESDIS at that time. (Our investigation is restricted to split-window equations which utilize brightness temperatures for channels 4 and 5 only, and not channel 3.)

Listed below are the tested algorithms, together with the date when each became operational. The nonlinear SST equations need a first guess of the sea surface temperature, T_{guess}. The NOAA recommendation is to use the 100-km analysed field temperature from the previous day. Since we could not provide this information, we

followed the NOAA alternative suggestion of generating the first guess by using the multichannel SST equations introduced at the same time as the nonlinear SST equations. T_4 and T_5 are the brightness temperatures (in K) for AVHRR channels 4 and 5; SST is the resulting temperature estimate in °C. The angle θ is the satellite zenith angle.

4.1. *MCSST: multichannel SST*

- NOAA-9 MCSST (16 July 1987)

$$\text{MCSST}_{9,\text{night}} = 3.6037T_4 - 2.6316T_5 - 0.27(T_4 - T_5)(\sec\theta - 1) \tag{8}$$

$$\text{MCSST}_{9,\text{day}} = 3.4317T_4 - 2.5062T_5 - 251.2163 \tag{9}$$

- NOAA-11 MCSST (17 November 1988)

$$\text{MCSST}_{11,\text{night}} = 0.9843T_4 + 2.0942(T_4 - T_5) + 2.0994(T_4 - T_5)(\sec\theta - 1)$$
$$- 1.1838(\sec\theta - 1) - 268.74 \tag{10}$$

$$\text{MCSST}_{11,\text{day}} = 0.9712T_4 + 2.0663(T_4 - T_5) + 1.8983(T_4 - T_5)(\sec\theta - 1)$$
$$- 1.9790(\sec\theta - 1) - 264.79 \tag{11}$$

- NOAA-12 MCSST (15 September 1994)

$$\text{MCSST}_{12,\text{night}} = 0.967077T_4 + 2.384376(T_4 - T_5)$$
$$+ 0.480788(T_4 - T_5)(\sec\theta - 1) - 263.94 \tag{12}$$

$$\text{MCSST}_{12,\text{day}} = 0.963563T_4 + 2.579211(T_4 - T_5)$$
$$+ 0.242598(T_4 - T_5)(\sec\theta - 1) - 263.006 \tag{13}$$

- NOAA-14 MCSST (20 March 1995)

$$\text{MCSST}_{14,\text{night}} = 2.275385(T_4 - T_5) + 1.029088T_4$$
$$+ 0.752567(T_4 - T_5)(\sec\theta - 1) - 282.24 \tag{14}$$

$$\text{MCSST}_{14,\text{day}} = 2.139588(T_4 - T_5) + 1.017342T_4$$
$$+ 0.779706(T_4 - T_5)(\sec\theta - 1) - 278.43 \tag{15}$$

Figure 2. DAT method: SST retrieval via atmospheric temperature tuning. (*a*) DWV failure. Tuning of the water vapour profile has failed to produce an $\text{SST}_4/\text{SST}_5$ intersection, indicating that the first-guess atmospheric temperature profile is in error. (*b*) DAT convergence. Water vapour profile is returned to first-guess values, and the atmospheric temperature is tuned. $\text{SST}_4/\text{SST}_5$ curves intersect when atmospheric temperature (in Kelvin) at each level has been scaled by multiplicative factor 0.965 (i.e. reduced by 3.5%), giving a DAT prediction of 13.1°C (the buoy reading was 13.8°C). (*c*) Initial and final atmospheric profiles. The reduction in atmospheric temperature has forced a lowering in water vapour amount at altitudes below 1.5 km and above 7 km. (At each level, relative humidity is not permitted to exceed 100%.) These curves apply to satellite pass m9n9 (18 May 1987).
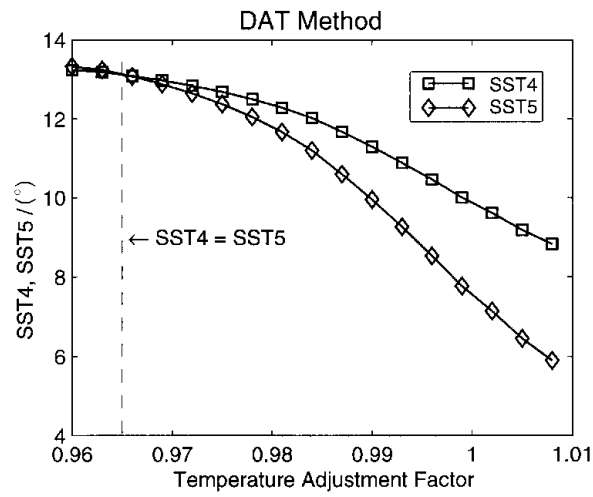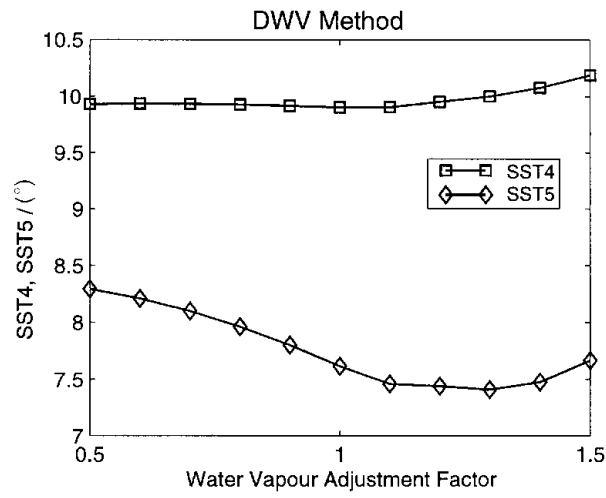
4.2. *CPSST: cross-product SST*

- NOAA-11 CPSST (2 March 1990)

$$\text{CPSST}_{11,\text{night}} = \frac{0.19817T_5 - 49.15}{0.20524T_5 - 0.17334T_4 - 6.10}(T_4 - T_5 + 1.47)$$

$$+ 0.96554T_5 + 0.96(T_4 - T_5)(\sec\theta - 1) + 267.13 \qquad (16)$$

$$\text{CPSST}_{11,\text{day}} = \frac{0.19410T_5 - 48.15}{0.20524T_5 - 0.17334T_4 - 6.25}(T_4 - T_5 + 1.32)$$

$$+ 0.94575T_5 + 0.60(T_4 - T_5)(\sec\theta - 1) + 260.99 \qquad (17)$$

4.3. *NLSST: nonlinear SST*

- NOAA-11 NLSST (10 April 1991)

$$\text{NLSST}_{11,\text{night}} = 0.96042T_4 + 0.087516T_{\text{guess}}(T_4 - T_5)$$

$$+ 0.852(T_4 - T_5)(\sec\theta - 1) - 261.46 \qquad (18)$$

$$\text{NLSST}_{11,\text{day}} = 0.94649T_4 + 0.08412T_{\text{guess}}(T_4 - T_5)$$

$$+ 0.751(T_4 - T_5)(\sec\theta - 1) - 257.20 \qquad (19)$$

where

$$T_{\text{guess}} = 1.02455T_4 + 2.45(T_4 - T_5)$$

$$+ 0.64(T_4 - T_5)(\sec\theta - 1) - 280.67 \qquad (20)$$

- NOAA-12 NLSST (15 September 1994)

$$\text{NLSST}_{12,\text{night}} = 0.888706T_4 + 0.081646T_{\text{guess}}(T_4 - T_5)$$

$$+ 0.576136(T_4 - T_5)(\sec\theta - 1) - 240.229 \qquad (21)$$

$$\text{NLSST}_{12,\text{day}} = 0.876992T_4 + 0.083132T_{\text{guess}}(T_4 - T_5)$$

$$+ 0.349877(T_4 - T_5)(\sec\theta - 1) - 236.667 \qquad (22)$$

where NOAA-12 MCSST equations (12) and (13) provided respective night and day values for T_{guess}.

- NOAA-14 NLSST (20 March 1995)

$$\text{NLSST}_{14,\text{night}} = 0.078095T_{\text{guess}}(T_4 - T_5) + 0.933109T_4$$

$$+ 0.738128(T_4 - T_5)(\sec\theta - 1) - 253.428 \qquad (23)$$

$$\text{NLSST}_{14,\text{day}} = 0.076066T_{\text{guess}}(T_4 - T_5) + 0.939813T_4$$

$$+ 0.801458(T_4 - T_5)(\sec\theta - 1) - 255.165 \qquad (24)$$

where NOAA-14 MCSST equations (14) and (15) provided respective night and day values for T_{guess}.

5. Test data set

Near-surface temperature data were obtained from a Datawell Waverider buoy moored off the west coast of Tasmania (145° 9.4′ E, 42° 8.7′ S) near the entrance to

Macquarie Harbour, 5 km from Cape Sorell, for the period 27 April to 21 December 1987. The calibration of the buoy was tested on two occasions which bracketed this period, and its accuracy was found to be better than ± 0.1 K with no evidence of any calibration drift (J. Reid 1992, personal communication). The effective depth of the buoy's temperature-sensing element was ~ 32 cm.

Coincident AVHRR images were inspected for this period and 34 cloud-free passes over the buoy region were selected. Channel-4 and -5 transmittances were computed using LOWTRAN-7 initialized with temporally proximate radiosonde profiles launched from Hobart, ~ 200 km southeast of the buoy. (Further details of the buoy and radiosonde data, and of the calibration and processing of the AVHRR data are given in Steyn-Ross *et al.* 1993.) To implement the H&M, Sob93 and Sob94 algorithms, the transmission ratio R_{54} was calculated from the LOWTRAN-computed transmittance values for the satellite-to-buoy slant path for each of the 34 satellite images.

6. Results

The comparative performance of the various algorithms was assessed in terms of bias, rms, and Q. The bias is the average value for the $(T_{Alg} - T_{buoy})$ difference,

$$\text{bias} = \frac{1}{N} \sum_{i=1}^{N} (T_{Alg, i} - T_{buoy, i}) \qquad N = 34 \tag{25}$$

and the rms is the standard deviation of these differences,

$$\text{rms} = \sqrt{\frac{1}{N-1} \sum_{i=1}^{N} (T_{Alg, i} - T_{buoy, i})^2} \tag{26}$$

where T_{Alg} is the surface temperature retrieved by the given algorithm. We define Q as an overall quality factor which combines the bias and rms error contributions in quadrature:

$$Q = \sqrt{\text{bias}^2 + \text{rms}^2} \tag{27}$$

The results for DWVT and the three variable-coefficient methods (H&M, Sob93, Sob94) are illustrated in figure 3 and listed in tables 1–4. In table 5 we list the results for the NESDIS fixed-coefficient formulas.

For the DWVT, H&M, Sob93, and Sob94 methods, we tested for sensitivity to temporal mismatch between the the time of satellite overpass and the time of sonde ascent. Sondes were launched from Hobart at 12-hourly intervals giving two atmospheric profiles per 24-hour period. We selected four sets of 34 candidate sondes to match up with the 34 AVHRR overpasses. The first sonde set was composed of those whose launch time most closely matched the satellite overpass time; the second set, labelled '10 before', were those sondes which were released 10 sonde-intervals earlier than the corresponding sondes in the 'closest' set; the third set ('10 after') were those sondes released 10 sonde-intervals later than the closest set. Because we felt that there might be an important difference between the daytime and night-time temperature profiles, we selected a fourth set of sondes which matched up night-time AVHRR passes with closest night-time sonde launch, and daytime AVHRR passes with closest daytime sonde launch (this set was labelled 'night/day'). The 'closest' and 'night/day' sets are not independent: about half of the entries in 'closest' are the same as those in 'night/day'. (Note that this sonde-age sensitivity test could not be
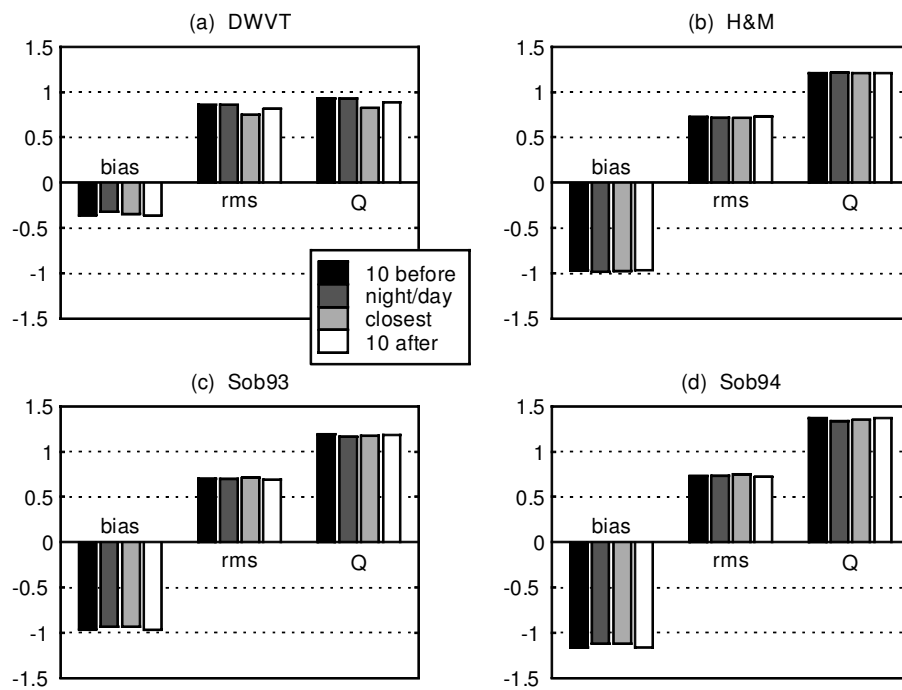
Figure 3. Comparison of algorithm performances for the Tasmanian dataset. Buoy temperature is taken as surface truth; bias and rms statistics show how well each algorithm recovers the buoy temperature. (*a*) DWVT accuracy is enhanced when the atmospheric sounding is recent ('night/day' and 'closest'), and degraded slightly when the sounding is stale ('10 before' and '10 after'). Transmittance-ratio methods of (*b*) H&M, (*c*) Sob93, and (*d*) Sob94 are less sensitive to age of atmospheric sounding. Best bias and Q statistics are returned by DWVT run with fresh soundings.

Table 1. DWVT statistics for 34 SST retrievals relative to buoy temperature. Data are in Kelvin, and are plotted in figure 3(*a*). Column headings indicate choice of radiosonde for first-guess atmosphere (see text).

Statistic	10-before	Night/day	Closest	10-after
Bias	− 0.36	− 0.32	− 0.34	− 0.36
rms	0.86	0.86	0.75	0.82
Q	0.93	0.93	0.82	0.89

Table 2. H&M statistics for 34 SST retrievals relative to buoy temperature. Data are plotted in figure 3(*b*).

Statistic	10-before	Night/day	Closest	10-after
Bias	− 0.97	− 0.98	− 0.98	− 0.96
rms	0.73	0.72	0.71	0.73
Q	1.21	1.22	1.21	1.21

applied to the NESDIS operational methods since these make no use of atmospheric profile information.)

Examining table 1 we see that DWVT shows a small sensitivity to sonde age,

Table 3. Sob93 statistics for 34 SST retrievals relative to buoy temperature. Data are plotted in figure 3(*c*).

Statistic	10-before	Night/day	Closest	10-after
Bias	− 0.96	− 0.93	− 0.93	− 0.97
rms	0.70	0.70	0.71	0.69
Q	1.19	1.17	1.18	1.19

Table 4. Sob94 statistics for 34 SST retrievals relative to buoy temperature. Data are plotted in figure 3(*d*).

Statistic	10-before	Night/day	Closest	10-after
Bias	− 1.16	− 1.12	− 1.12	− 1.16
rms	0.73	0.73	0.75	0.72
Q	1.37	1.34	1.35	1.37

Table 5. SST error statistics for the selected test set of NESDIS operational algorithms. SST retrieval was performed by applying the 34 (T_4, T_5) pairs of 1987 NOAA-9 brightness temperatures to each of the fixed-coefficient equations listed in §4. The method acronym and subscript identifies the equations used, thus $MCSST_9$ indicates multichannel SST using NOAA-9 equations (8) (night passes) and (9) (day passes). The NLSST equations were tested twice: once using the T_{guess} equations listed in §4 (e.g. $NLSST_{11}$), then a second time using NOAA-9 MCSST to provide the first guess (e.g. $NLSST_{11,9}$). Rank identifies the three best results as measured by the Q-statistic.

Method	Bias	rms	Q	Rank
$MCSST_9$	− 0.01	0.64	0.64	1
$MCSST_{11}$	− 1.07	0.62	1.23	
$MCSST_{12}$	− 0.89	0.65	1.10	
$MCSST_{14}$	− 1.27	0.68	1.44	
$CPSST_{11}$	− 1.25	0.70	1.43	
$NLSST_{11}$	− 1.02	0.72	1.25	
$NLSST_{11,9}$	− 0.94	0.71	1.17	
$NLSST_{12}$	− 0.26	0.70	0.75	3
$NLSST_{12,9}$	− 0.21	0.70	0.73	2
$NLSST_{14}$	− 0.93	0.71	1.17	
$NLSST_{14,9}$	− 0.85	0.70	1.10	

with rms error worsening by $\sim 0.1\,K$ when the method was run with atmospheric profiles derived from sondes launched five days early (i.e. 10 sonde-intervals before) or five days late (10 sonde-intervals after). This age sensitivity also shows up as a slight concavity in the bias, rms, and Q error bars of figure 3(*a*). Both Sob93 and Sob94 exhibit slight age sensitivity in their respective bias results (figure 3(*c*), 3(*d*)), while H&M retrievals seem to be independent of sonde age.

Comparing the relative performances of the four tuned-atmosphere algorithms (tables 1–4), all methods returned a negative bias (i.e. retrieved temperature under-estimated buoy temperature). This is consistent with the skin sea temperature being cooler than the bulk sea temperature sensed by the buoy thermistor at depth 32 cm.

All four methods had similar rms statistics, though the more 'complex' algorithms tend to show larger rms error (~ 0.71 K for H&M and Sob93; ~ 0.75 K for Sob94 and DWVT). Because the bias error for DWVT was much smaller than for the others, the summary Q-statistic reported DWVT as the best performer among the tuned-atmosphere algorithms.

Turning now to the NESDIS operational results, table 5 shows that MCSST for NOAA-9 gives excellent retrievals with a near-zero bias and an rms error of 0.64 K. With one exception (NLSST for NOAA-12), we find that applying the NOAA-9 brightness temperature data to the SST equations for the later satellites produces notably degraded bias values. This degradation is not unexpected, since the regression equations encapsulate the average atmospheric state prevailing at the time of the regression experiments, and this average atmospheric state changes with time. Also, the channel-4 and -5 filter functions for the NOAA satellites are similar, but not identical; however, the filter function effect on algorithm accuracy is probably minor. We note that all three NLSST statistics are improved when $MCSST_9$ values are used for the first guess; this is not surprising since it is simply underscoring the importance of an accurate first guess seed for the nonlinear method.

It is interesting to observe that the rms statistics for the NESDIS formulas confirm the trend observed in the tuned-atmosphere methods: rms error increases with algorithm complexity.

7. Discussion and conclusions

The use of the R_{54} transmittance ratio requires knowledge of the atmospheric state. It is often the case that local radiosondes are not available. Kleespies and McMillin (1990), and Jedlovec (1990) introduced the concept of using ratios of the spatial variance of the brightness temperatures to determine atmospheric and surface parameters. This idea was expanded by Harris and Mason (1992) for SSTs and by Sobrino *et al.* (1994) for LSTs. Barton (1995) investigated these variance methods and found that while they work on simulated satellite data, they are quite unstable when applied to real satellite data. In addition, because our surface data were provided by a buoy which was moored only a few km from the Tasmanian coast, it is not feasible to compute a spatial variance measure for the region centred on the buoy which is guaranteed to be uncontaminated by nearby land pixels. For these reasons we elected not to use the variance method to estimate R_{54}, since it is likely that the performance of the R_{54}-based algorithms would have been compromised.

When a split-window SST algorithm is developed, the aim is to produce a single-line equation whose accuracy is independent of atmospheric state. (As pointed out by a reviewer, there is no reason why one could not develop a suite of such single-line equations for different atmospheric states which, for example, might depend on latitude or viewing angle. However, this is not current practice.) Any single-line algorithm will work best when the prevailing atmospheric conditions are similar to some average atmospheric state defined by the suite of sondes/buoys/satellite data used to craft the algorithm. The resulting regression coefficients represent the best-fit curve which maps at-satellite brightness temperature to surface temperature through this notional average atmosphere. However, when the prevailing atmospheric conditions are significantly different, the performance of regression-based algorithm would be expected to suffer. H&M, Sob93, Sob94, and the NESDIS suite are all regression-based methods.

The underlying philosophy of DWVT is quite different: DWVT does not use

regression to relate brightness temperature to surface temperature, and is not confined in its applicability to one particular region or average atmosphere. Instead, it starts with a first-guess atmosphere whose profile is then tuned iteratively, using the equations of transfer, in a quest to find a pair of consistent SST estimates. When applied to the Tasmanian dataset, DWVT retrievals exhibited slightly greater noise (rms error) but significantly better accuracy (smaller bias) than the H&M, Sob93 and Sob94 family of R_{54}-based algorithms. When compared with the NESDIS operational formulas, DWVT was outperformed by $MCSST_9$ and $NLSST_{12}$. The excellent results of $MCSST_9$ indicate that the standard regression methods work very well in situations of low water vapour loading; we have not been able to test relative performances in tropical situations where the water vapour column could be significant, though we would expect a DWVT approach to work well.

We found that the DWVT method returned minimum bias and rms errors (i.e. optimum performance) when the temporally closest sondes were used, and a slightly degraded performance when positively or negatively aged sondes were selected, indicating the importance of a reasonable first guess for the atmospheric state.

We believe that DWVT has potential for improved accuracy. We are presently researching techniques which would allow the profiles for water vapour and atmospheric temperature to be tuned simultaneously, rather than sequentially as at present. Progress along these lines is reported in Jelenak *et al.* (1998).

Acknowledgments

We thank John Reid and Paul Tildesley of CSIRO Marine Laboratories, Hobart, Australia; John for providing both the buoy dataset and the initial motivation to develop a more accurate SST retrieval methodology, and Paul for extracting and processing the AVHRR imagery. We also acknowledge the very useful comments from two anonymous referees.

Appendix. Rationale for dynamic atmospheric tuning

For a clear-sky view of an ocean pixel of skin temperature T_s, the thermal signal I arriving at the satellite radiometer is the sum of the surface-generated intensity, attenuated by the intervening atmosphere, plus the upwelling intensity radiated by the atmosphere itself. For radiometer channel k ($k=4$, 5 for AVHRR), the radiance will be

$$I_k = B_k(T_s)\tau_k + B_k(\bar{T}_a)(1-\tau_k) \tag{A1}$$

where $B_k(T_s)$ is the Planck function in channel k evaluated at the surface temperature; $B_k(\bar{T}_a)$ is the Planck function at average atmospheric temperature $\bar{T}_a$; τ_k is the total atmospheric transmittance in channel k, and we have assumed the sea surface has unit emissivity. $\bar{T}_a$ is an effective atmospheric temperature obtained by inverting the summed transmittance-weighted atmospheric radiances at each level i:

$$B_k(\bar{T}_a) = \frac{\int_{\tau_k}^{1} B_k(T_a)\,\mathrm{d}\tau'}{\int_{\tau_k}^{1} \mathrm{d}\tau'} \approx \frac{\Sigma_i B_k(T_{a,i})\cdot(\Delta\tau_i)_k}{1-\tau_k} \tag{A2}$$

where $\Delta\tau_i$ is the change in transmittance, relative to the top of the atmosphere, across level i. Strictly, the two AVHRR thermal channels will have distinct average

atmospheric temperatures, but in practice we find that these two averages are closely similar, typically differing by no more than $1\,K$ over the 6-month period of the present study.

For the DWVT algorithm we invert equation (A1) to give a pair of surface temperature estimates, one for each channel,

$$\text{SST}_k \equiv T_{s,k} = B_k^{-1}\left[\frac{I_k - B_k(\bar{T}_a)(1 - \tau_k)}{\tau_k}\right] \quad\quad (A3)$$

where the operator on the square brackets is the inverse Planck function. In constrast, the split-window algorithms work directly with the at-satellite radiance I_k to give apparent brightness temperatures T_k,

$$T_k = B_k^{-1}[I_k] = \frac{c_2\,\nu_k}{\log_e(1 + c_1\,\nu_k^3/I_k)} \qu\quad (A4)$$

where ν_k is the channel central wavenumber for channel k, and c_1 and c_2 are the first and second radiation constants. For radiance expressed in standard NOAA units $[\text{mW}/(\text{m}^2\,\text{sr}\,\text{cm}^{-1})]$, the first and second radiation constants are respectively $c_1 = 1.191 \times 10^{-5}\,\text{cm}^3\,\text{mW}/(\text{m}^2\,\text{sr}\,\text{cm}^{-1})$, and $c_2 = 1.439 \times 10^2\,\text{cm}\,K$.

If the atmospheric state is known precisely, from, e.g. a coincident radiosounding, then equation (A3) gives two independent retrievals for T_s, one for each channel. In the more usual case, knowledge of the atmosphere is imperfect, being estimated from a nearby sounding or from a climatology. Thus the two surface temperature estimates, SST_4 and SST_5, would not be expected to agree, either because of error in the assumed water vapour profile, or in the assumed atmospheric temperature profile, or in both. The obvious question is then: how should the first-guess profile be adjusted in order to give a good surface temperature retrieval? And second: is the vertical structure of the profile important?

In the context of the mean-value approximation for $\bar{T}_a$, the radiative transfer equation depends only on the transmittance $\tau = \exp(-kU)$ where k is the absorption coefficient, and U is the total water vapour amount. To the extent that $\bar{T}_{a4} = \bar{T}_{a5}$, the unknowns in the equation of transfer are only U, $\bar{T}_a$ and T_s. The equation does not depend on the fine structure of the atmosphere. Thus in principle, one need only vary the total water vapour amount and/or the average atmospheric temperature to solve for the surface temperature. This can be achieved by a simple shift of either the water vapour profile (by a fixed fraction at each level) or the atmospheric temperature profile. This is the underlying philosophy of DWVT.

References

BARTON, I. J., 1995, Satellite-derived sea surface temperatures–current status. *Journal of Geophysical Research*, **15**, 8777–8790.

CHAHINE, M. T., 1970, Inverse problems in radiative transfer: Determination of atmospheric parameters. *Journal of the Atmospheric Sciences*, **27**, 960–967.

EYRE, J. R., 1987, On systematic errors in satellite sounding products and their climatological mean values. *Quarterly Journal of the Royal Meteorological Society*, **113**, 279–292.

EYRE, J. R., 1989, Inversion of cloudy satellite sounding radiances by nonlinear optimal estimation I: Theory and simulation for TOVS. *Quarterly Journal of the Royal Meteorological Society*, **115**, 1001–1026.

HAN, Y., SHAW, J. A., CHURNSIDE, J. H., BROWN, P. D., and CLOUGH, S. A., 1997, Infrared spectral radiance measurements in the tropical pacific atmosphere. *Journal of Geophysical Research*, **102**, 4353–4356.

HARRIS, A. R., and MASON, I. M., 1992, An extension to the split-window technique giving improved atmospheric correction and total water vapour. *International Journal of Remote Sensing*, **13**, 881–892.

JEDLOVEC, G. J., 1990, Precipitable water estimation from high-resolution split window radiance measurements. *Journal of Applied Meteorology*, **29**, 863–877.

JELENAK, A., STEYN-ROSS, M., and STEYN-ROSS, D. A., 1998, Simultaneous tuning of water vapour and atmospheric temperature for determination of sea surface temperature from AVHRR. In *9th Australasian Remote Sensing and Photogrammetry Conference, Sydney, Australia,* vol. 1, CD-ROM, paper 65.

KLEESPIES, T. J., and MCMILLIN, L. M., 1990, Retrieval of precipitable water from observations in the split-window over varying surface temperatures. *Journal of Applied Meteorology*, **29**, 851–862.

KNEIZYS, F. X., SHETTLE, E. P., ABREU, L. W., CHETWYND, J. H., ANDERSON, G. P., GALLERY, W. O., SELBY, J. E. A., and CLOUGH, S. A., 1988, Users guide to LOWTRAN-7, Technical Report AFGL-TR-88-0177, Opt./Infrared Technol. Div., U.S. Air Force Geophys. Lab., Hanscom Air Force Base, Massachusetts.

MCMILLIN, L. M., 1975, Estimation of sea surface temperatures from two infrared window measurements with different absorption. *Journal of Geophysical Research*, **80**, 5113–5117.

PRATA, A. J., 1993, Land surface temperatures derived from the AVHRR and ATSR, 1, Theory. *Journal of Geophysical Research*, **98**, 16,689–16,702.

RODGERS, C. D., 1976, Retrieval of atmospheric temperature and composition from remote measurements of thermal radiation. *Reviews of Geophysics and Space Physics*, **14**, 609–624.

SMITH, W. L., 1970, Iterative solution of the radiative transfer equation for temperature and absorbing gas profile of an atmosphere. *Applied Optics*, **9**, 1993–1999.

SOBRINO, J. A., LI, Z.-L., and STOLL, M. P., 1993, Impact of the atmospheric transmittance and total water vapor content in the algorithms for estimating sea surface temperatures. *IEEE Transactions on Geoscience and Remote Sensing*, **31**, 946–958.

SOBRINO, J. A., LI, Z.-L., STOLL, M. P., and BECKER, F., 1994, Improvements in the split-window technique for land surface temperature determination. *IEEE Transactions on Geoscience and Remote Sensing*, **32**, 243–253.

STEYN-ROSS, M. L., STEYN-ROSS, D. A., SMITH, P. J., SHEPHERD, J. D., REID, J., and TILDESLEY, P., 1993, Water vapor correction method for advanced very high resolution radiometer data. *Journal of Geophysical Research*, **98**, 22,817–22,826.

STEYN-ROSS, M. L., STEYN-ROSS, D. A., and EMERY, W. J., 1997, A dynamic water vapor correction method for the retrieval of land surface temperatures from the advanced very high resolution radiometer. *Journal of Geophysical Research*, **102**, 19,629–19,643.

STREBEL, D. E., LANDIS, D. R., HUEMMRICH, K. F., and MEESON, B. W., 1994, *Collected Data of the First ISLSCP Field Experiment, vol. 1, Surface Observations and Non-image Data Sets* [CD-ROM] (NASA, Washington, DC).

STREBEL, D. E., LANDIS, D. R., NEWCOMER, J. N., VAN ELBURG-OBLER, D., MEESON, B. W., and AGBU, P. A., 1992, *Collected Data of the First ISLSCP Field Experiment, vol. 2, Satellite Imagery, 1978–1989* [CD-ROM] (NASA, Washington, DC).